

Continual Multimodal Egocentric Activity Recognition via Modality-Aware Novel Detection

Wonseon Lim^{1†} Hyejeong Im^{1†} Dae-Won Kim^{1*}

¹School of Computer Science and Engineering, Chung-Ang University

{costor, ihj2207, dwkim}@cau.ac.kr

Abstract

Multimodal egocentric activity recognition integrates visual and inertial cues for robust first-person behavior understanding. However, deploying such systems in open-world environments requires detecting novel activities while continuously learning from non-stationary streams. Existing methods rely on the main logits for novelty scoring, without fully exploiting the complementary evidence available from individual modalities. Because these logits are often dominated by RGB, cues from other modalities, particularly IMU, remain underutilized, and this imbalance worsens over time under catastrophic forgetting. To address this, we propose MAND, a modality-aware framework for multimodal egocentric open-world continual learning. At inference, Modality-aware Adaptive Scoring (MoAS) estimates sample-wise modality reliability from energy scores and adaptively integrates modality logits to better exploit complementary modality cues for novelty detection. During training, Modality-wise Representation Stabilization Training (MoRST) preserves modality-specific discriminability across tasks via auxiliary heads and modality-wise logit distillation. Experiments on a public multimodal egocentric benchmark show that MAND improves novel activity detection AUC by up to 10% and known-class classification accuracy by up to 2.8% over state-of-the-art baselines.

1. Introduction

Egocentric activity recognition has become a cornerstone of embodied AI, enabling assistive perception, AR/VR interaction, and life-logging applications [11, 13, 29]. Unlike third-person vision, egocentric perception provides first-person sensory cues that reflect the wearer’s intent and motion [8]. Multimodal egocentric activity recognition (MMEA), which integrates RGB and inertial measurement unit (IMU) streams, provides complementary spatial and

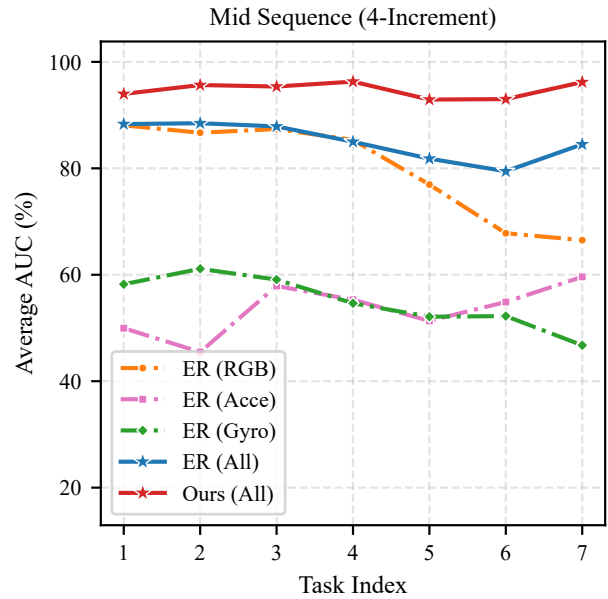


Figure 1. Task-wise average AUC for novel activity detection in the mid-sequence setting. ER (All), which uses all modalities, closely tracks the RGB-only baseline, indicating that its main logits are largely dominated by RGB. In contrast, MAND maintains consistently higher performance by better exploiting modality-specific evidence.

kinematic cues for robust, temporally grounded activity understanding [12]. However, real-world deployment of MMEA requires models to detect novel activities while continually learning from sequential task streams.

Recent works have extended MMEA to continual learning (CL) settings [7, 15, 36], yet most still operate under the closed-world assumption, where the label space is fixed and only known classes appear at test time. In real-world egocentric streams, unseen activities naturally appear over time, and models must detect novel activities while incrementally recognizing known ones in non-stationary data streams [22, 24]. This open-world continual learning (OWCL) setting further

[†]Equal contribution.

^{*}Corresponding author.

complicates MMEA, as the model must both fuse heterogeneous modalities for robust recognition and distinguish novel activities from known ones, while continually adapting without catastrophic forgetting.

A recent effort, MONET [5], advances multimodal egocentric OWCL by incorporating modality-specific heads and pseudo-OOD-based dynamic thresholds into an online continual learning pipeline. However, MONET relies solely on the main logits for novelty scoring, without leveraging the modality-specific evidence encoded in individual RGB and IMU logits. These logits capture complementary spatial and kinematic cues, respectively. Because the main logits are primarily driven by RGB, the resulting novelty scores can underrepresent the discriminative contribution of other modalities, particularly IMU, as illustrated in Fig. 1. This imbalance becomes more pronounced over time, as IMU is more susceptible to catastrophic forgetting, further degrading its discriminability and reducing separability between known and novel activities.

To address this, we propose MAND, a modality-aware framework for multimodal egocentric OWCL that tackles the problem through two complementary components. At inference, *Modality-aware Adaptive Scoring* (MoAS) estimates a sample-wise reliability weight for each modality from its energy score and adaptively integrates weighted modality logits into the main logits, thereby better exploiting complementary modality cues for novelty detection. During training, *Modality-wise Representation Stabilization Training* (MoRST) equips each modality encoder with a lightweight classification head and preserves per-modality decision boundaries across tasks via modality-specific logit distillation on replayed exemplars. By preserving discriminative per-modality prediction scores throughout the task stream, MoRST enables MoAS to leverage more stable modality-specific signals for better-calibrated novelty estimation at inference.

Extensive experiments on a public multimodal egocentric benchmark demonstrate the effectiveness of the proposed method. Across all sequence-length settings, MAND improves novel activity detection AUC by up to 10% and known activity accuracy by up to 2.8% over state-of-the-art baselines. These results show that combining modality-aware inference with modality-wise stabilization improves both novelty detection and incremental recognition in multimodal egocentric OWCL. The main contributions are summarized as follows:

- We show that relying solely on the main logits for novelty scoring underutilizes per-modality discriminative signals, and that this limitation arises from modality dominance and is further aggravated by modality-wise forgetting under incremental learning.
- We propose MoAS, an inference-time module that estimates sample-wise modality reliability from energy scores

and adaptively integrates modality logits to better exploit complementary modality cues for novelty scoring.

- We propose MoRST, a training-time module that preserves per-modality decision boundaries through modality-specific heads and logit distillation, thereby maintaining consistent per-modality prediction scores across tasks.

2. Related Work

2.1. Multimodal Egocentric Activity Recognition

Human activity recognition has long benefited from fusing visual and inertial cues [6, 30]. More recently, large-scale egocentric datasets such as EPIC-KITCHENS [8], Ego4D [13], and ActionSense [9] have enabled first-person activity understanding with synchronized RGB-IMU streams. UESTC-MMEA-CL [36] introduced the first multimodal egocentric benchmark for continual learning, together with a multimodal baseline evaluated using representative CL methods such as LwF [25], EWC [23], and iCaRL [32]. CMR-MFN [34] models evolving cross-modal correlations using an expandable architecture with confusion mixup regularization. AID [7] addresses modality imbalance by enhancing sensor features through vision-sensor attention. FGVR [15] further improves long-term continual learning by reducing modality imbalance and promoting more generalizable multimodal representations. These studies highlight the importance of maintaining balanced and consistent modality representations in multimodal continual learning. Despite these advances, existing MMEA-CL methods remain confined to the closed-world assumption, and thus cannot detect unseen activities that naturally arise in real-world egocentric streams. Unlike prior MMEA-CL methods, our work considers an open-world continual learning setting in which the model must jointly perform novel activity detection and known-class recognition.

2.2. Open-World Continual Learning

Continual learning (CL) seeks to mitigate catastrophic forgetting through regularization, architectural expansion, or exemplar replay [28, 32, 37], but typically assumes a fixed label space that precludes detecting unseen categories. Open-world recognition [1, 35] highlights the need to jointly detect novel classes and retain prior knowledge, giving rise to *Open-World Continual Learning* (OWCL) [26]. Joseph et al. [19] identify unknown objects via contrastive clustering in an incremental detection setting. Kim et al. [22] further establish novelty detection as a theoretical prerequisite for stable class-incremental learning, enabling self-initiated discovery and fast adaptation. MORE [21] and SHELS [14] pursue representational disentanglement and feature exclusivity for novelty-aware CL, while Pro-KT [24] transfers open-world knowledge through structured prototype evolution. All of these methods, however, target unimodal image streams.

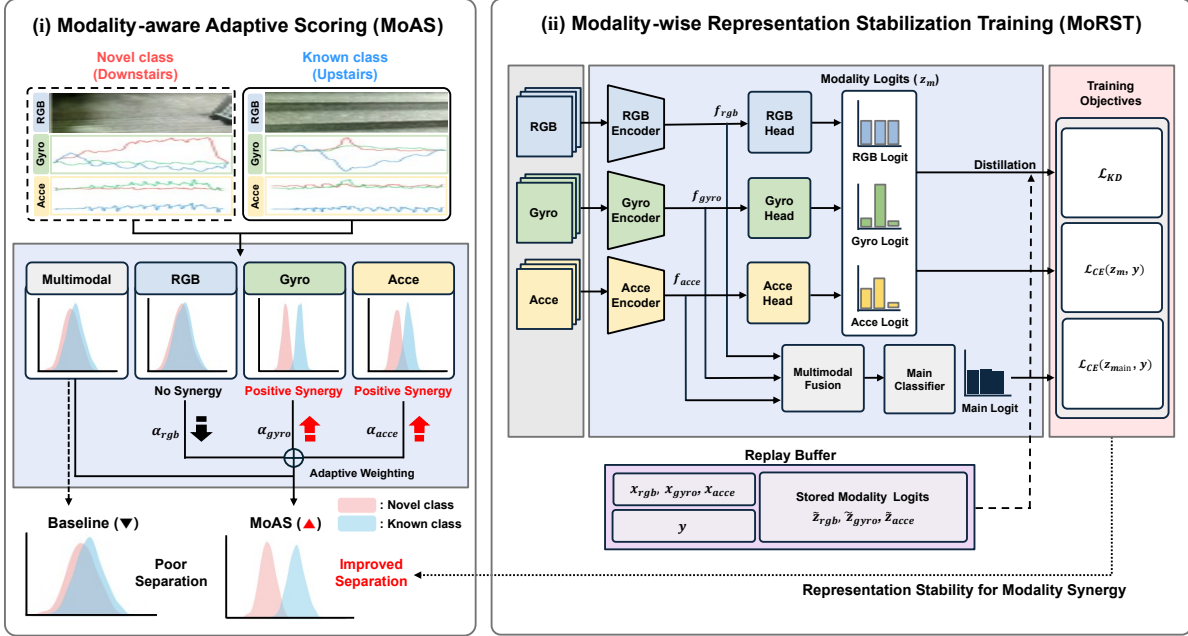


Figure 2. Overview of our modality-aware framework for MMEA OWCL. **Left (MoAS, inference):** per-sample modality reliabilities are estimated from normalized energy scores and used to adaptively integrate weighted modality logits with the main logits, improving separability between known and novel activities. **Right (MoRST, training):** modality-specific heads and replay-based modality-logit distillation preserve per-modality decision boundaries across tasks. MoRST stabilizes modality-specific evidence over time, which MoAS then leverages to produce better-calibrated novelty scores.

MONET [5] is the first to extend OWCL to multimodal egocentric settings, combining online replay with pseudo-OOD thresholds and EMA-based distillation. However, its novelty scoring relies solely on the main logits, without leveraging complementary modality-specific evidence from individual modalities, and it does not explicitly address modality-wise forgetting under sequential updates. In contrast, our work addresses both limitations by exploiting per-modality prediction signals for novelty scoring at inference and preserving modality-specific representations throughout continual learning.

3. Method

3.1. Preliminary

We study multimodal egocentric activity recognition [36] under an open-world continual learning (OWCL) protocol [22, 24]. The learner is trained sequentially on a stream of class-incremental tasks $\{\mathcal{D}_t\}_{t=1}^T$, where each task introduces labeled samples from newly observed classes and expands the label space $\mathcal{Y}_0 \subset \mathcal{Y}_1 \subset \dots \subset \mathcal{Y}_T$. Each training sample consists of three modalities, $x = \{x_{rgb}, x_{gyro}, x_{acce}\}$, with label $y \in \mathcal{Y}_t$. After learning task t , a test sample may belong either to a known class in \mathcal{Y}_t or to a novel class outside \mathcal{Y}_t , requiring the model to jointly perform novelty detection and known-class recognition under non-stationary

multimodal streams.

We adopt a standard multimodal encoder–fusion–classifier architecture [20, 36]. Given the modality set $\mathcal{M} = \{rgb, gyro, acce\}$, each modality encoder $F_m(\cdot)$ produces an embedding $f_m = F_m(x_m)$, and a fusion module $G(\cdot)$ aggregates them into a fused representation $f_{main} = G(\{f_m\}_{m \in \mathcal{M}})$. The main classifier $C(\cdot)$ then outputs main logits $z_{main} = C(f_{main})$ for known-class recognition. In addition, we equip each modality encoder with a modality-specific head $H_m(\cdot)$ that outputs modality-specific logits $z_m = H_m(f_m)$, which are used for modality-aware novelty scoring and modality-wise stabilization. These heads are introduced only in methods that explicitly rely on modality-specific predictions, namely MONET [5] and our method.

3.2. Modality-Aware Novelty Detection and Training

We propose MAND, a modality-aware framework for multimodal egocentric OWCL, which consists of two complementary components: (i) Modality-aware Adaptive Scoring (MoAS) for novelty detection at inference time, and (ii) Modality-wise Representation Stabilization Training (MoRST) for continual learning during training. As illustrated in Fig. 2, MoAS improves separability between known and novel activities by adaptively calibrating the main logits using modality-specific evidence, while MoRST suppresses

Algorithm 1 Modality-aware Adaptive Scoring

- 1: **Input:** Sample $x = \{x_m\}_{m \in \mathcal{M}}$, encoders $\{F_m\}_{m \in \mathcal{M}}$, heads $\{H_m\}_{m \in \mathcal{M}}$, fusion G , classifier C , buffer statistics $\{(\mu_m, \sigma_m)\}_{m \in \mathcal{M}}$
- 2: **Output:** Novelty score $s(x)$
- 3: **for** $m \in \mathcal{M}$ **do**
- 4: $f_m \leftarrow F_m(x_m)$
- 5: $z_m \leftarrow H_m(f_m)$
- 6: $E_m \leftarrow -\log(\sum_c \exp(z_{m,c}))$
- 7: $r_m \leftarrow -(E_m - \mu_m)/\sigma_m$
- 8: **end for**
- 9: $f_{\text{main}} \leftarrow G(\{f_m\}_{m \in \mathcal{M}})$
- 10: $z_{\text{main}} \leftarrow C(f_{\text{main}})$
- 11: $\alpha_m \leftarrow \exp(r_m) / \sum_{j \in \mathcal{M}} \exp(r_j)$ for $m \in \mathcal{M}$
- 12: $z_c^{\text{MoAS}} \leftarrow z_{\text{main},c} + \sum_{m \in \mathcal{M}} \alpha_m \cdot z_{m,c}$ for all classes c
- 13: $s(x) \leftarrow \max_c z_c^{\text{MoAS}}$

modality-wise representation drift through modality-specific heads and modality-specific logit distillation.

3.2.1. Modality-aware Adaptive Scoring

In open-world multimodal streams, the main logits z_{main} can be overly dominated by a single high-confidence modality, suppressing complementary evidence from other modalities and reducing separability between known and novel activities. To mitigate this modality dominance and better exploit complementary modality cues, we introduce Modality-aware Adaptive Scoring (MoAS). MoAS computes a sample-wise reliability score for each modality from its modality-specific head and adaptively integrates weighted modality logits into z_{main} .

We first estimate the sample-wise reliability of each modality using an energy score computed from its modality-specific logits. For modality m , the energy is defined as

$$E_m(x) = -\log \sum_c \exp(z_{m,c}(x)) \quad (1)$$

Lower energy indicates stronger modality-specific evidence for the input. However, raw energy values are not directly comparable across modalities because each encoder produces logits with different characteristic scales. As a result, raw energy may reflect modality-specific logit magnitude rather than true per-sample reliability.

To obtain reliability scores that are comparable across modalities, we normalize each modality's energy using the statistics computed on the replay buffer \mathcal{B} . Specifically, we compute per-modality energy mean μ_m and standard deviation σ_m over the exemplars, and define the reliability score as:

$$r_m(x) = -\frac{E_m(x) - \mu_m}{\sigma_m} \quad (2)$$

Here, r_m measures how strongly modality m responds to

Algorithm 2 Modality-wise Representation Stabilization Training

- 1: **Input:** Training data \mathcal{D}_t , replay buffer \mathcal{B} , modalities \mathcal{M} , head loss weight λ , distillation weight β
- 2: **Initialize:** Model parameters θ
- 3: **for** mini batch in \mathcal{D}_t **do**
- 4: $(x, y) \leftarrow \text{mini batch} \cup \mathcal{B}$
- 5: $\{\tilde{z}_m\}_{m \in \mathcal{M}} \leftarrow \mathcal{B}$
- 6: $f_m \leftarrow F_m(x_m)$ for all $m \in \mathcal{M}$
- 7: $f_{\text{main}} \leftarrow G(\{f_m\}_{m \in \mathcal{M}})$
- 8: $z_{\text{main}} \leftarrow C(f_{\text{main}})$
- 9: $z_m \leftarrow H_m(f_m)$ for all $m \in \mathcal{M}$
- 10: $\mathcal{L}_{\text{Sup}} \leftarrow \mathcal{L}_{\text{CE}}(z_{\text{main}}, y) + \lambda \cdot \frac{1}{|\mathcal{M}|} \sum_{m \in \mathcal{M}} \mathcal{L}_{\text{CE}}(z_m, y)$
- 11: $\mathcal{L}_{\text{KD}} \leftarrow \sum_{m \in \mathcal{M}} \|\tilde{z}_m - z_m\|_2^2$
- 12: $\mathcal{L} \leftarrow \mathcal{L}_{\text{Sup}} + \beta \cdot \mathcal{L}_{\text{KD}}$
- 13: $\theta \leftarrow \text{Optimizer}(\nabla \mathcal{L}, \theta)$
- 14: **end for**

a given sample relative to its own energy distribution, with higher values indicating stronger modality-specific evidence. This normalization compensates for cross-modality scale differences and makes reliability scores directly comparable.

We then derive modality weights $\alpha_m(x)$ by applying a softmax over the reliability scores:

$$\alpha_m(x) = \frac{\exp(r_m(x))}{\sum_{j \in \mathcal{M}} \exp(r_j(x))} \quad (3)$$

These weights adaptively rebalance modality contributions by reducing dominance from a single modality and increasing the influence of complementary modalities.

To compute the final prediction logits, we refine the main logits by aggregating the modality-weighted logits. We define the combined logit vector as

$$z_c^{\text{MoAS}}(x) = z_{\text{main},c}(x) + \sum_{m \in \mathcal{M}} \alpha_m(x) z_{m,c}(x) \quad (4)$$

We then compute the novelty score using the MaxLogit criterion:

$$s(x) = \max_c z_c^{\text{MoAS}}(x) \quad (5)$$

We provide the MoAS inference procedure in Algorithm 1.

3.2.2. Modality-wise Representation Stabilization Training

The effectiveness of MoAS depends on the quality of per-modality evidence, which can degrade under continual updates. In particular, non-dominant modalities such as IMU are more susceptible to catastrophic forgetting than RGB-dominant fused predictions. This gradually reduces modality-specific discriminability and weakens the reliability of modality-aware scoring over the task stream. To preserve discriminative per-modality evidence throughout

continual learning, we propose Modality-wise Representation Stabilization Training (MoRST). During training, we jointly optimize the main classifier and modality-specific heads using the following objective:

$$\mathcal{L}_{\text{Sup}} = \mathcal{L}_{\text{CE}}(z_{\text{main}}, y) + \lambda \cdot \frac{1}{|\mathcal{M}|} \sum_{m \in \mathcal{M}} \mathcal{L}_{\text{CE}}(z_m, y) \quad (6)$$

where \mathcal{L}_{CE} denotes the cross-entropy loss and λ controls the contribution of modality-specific supervision. This auxiliary supervision encourages each modality encoder to preserve class-discriminative structure in its own feature space, rather than relying solely on the dominant fused representation.

To further preserve modality-specific decision information across tasks, we store modality-specific logits together with replay exemplars in the buffer. For each exemplar $(\tilde{x}, \tilde{y}) \in \mathcal{B}$, we maintain stored modality-specific logits $\tilde{z}_m \in \mathcal{M}$, where \tilde{z}_m denotes the previously recorded logits of modality m for the same sample. Unlike standard logit replay [2], which matches a single fused output, MoRST penalizes deviations between each modality head and its own stored logits independently:

$$\mathcal{L}_{\text{KD}} = \sum_{m \in \mathcal{M}} \|\tilde{z}_m - z_m\|_2^2 \quad (7)$$

This per-modality matching helps each modality encoder retain its own class-discriminative structure, yielding more stable modality-specific prediction signals for the energy-based reliability estimation in MoAS. The final training objective is

$$\mathcal{L} = \mathcal{L}_{\text{Sup}} + \beta \cdot \mathcal{L}_{\text{KD}} \quad (8)$$

with β controlling the strength of modality-specific logit preservation. This distillation stabilizes modality-specific predictions over time, enabling more consistent modality reliability estimation during MoAS inference. Algorithm 2 summarizes the full training procedure.

4. Experiments

4.1. Experimental Setup

Datasets and Metrics. We evaluate the proposed method on UESTC-MMEA-CL [36], a multimodal egocentric benchmark consisting of RGB, gyroscope, and accelerometer streams over 32 activity classes. We follow both the novel activity detection and known-class incremental learning protocols. For novelty detection [24], we report the area under the ROC curve (AUC_{T}) and the false positive rate at 95% true positive rate ($\text{FPR}_{95\text{T}}$). For known-class continual recognition [22], we report the average accuracy (ACC_{T}) and forgetting (FGT_{T}) across all tasks.

Comparing methods. We compare MAND against representative methods for both novelty scoring and contin-

ual known-class recognition. For novelty scoring, we consider widely used post-hoc methods, including MSP [16], MaxLogit [17], Entropy [3], and Energy [27]. For continual known-class learning, we evaluate representative replay-based methods, including iCaRL [32], ER [4], DER++ [2], and Foster [33], as well as multimodal CL methods, including CMR-MFN [34] and MONET [5]. For Table 1, each CL method is paired with each novelty scoring function. Unlike the baseline combinations, MAND is evaluated as a unified framework that jointly performs continual learning and modality-aware novelty scoring.

Implementation details. For the backbone architecture, we use BN-Inception [18], pretrained on ImageNet [10], for the RGB modality, and DeepConvLSTM [31] for the IMU modalities to capture both short- and long-term motion dynamics. All modalities are temporally aligned and fused using a Temporal Binding Network (TBN) [20], and the fused features are fed into the classifier. Following UESTC-MMEA-CL [36], we adopt modality-specific optimizers and hyperparameters. The RGB encoder is optimized with SGD, while the IMU encoders are optimized with RMSProp, both with an initial learning rate of 0.001. Each task is trained for 50 epochs, and the learning rate is decayed by a factor of 10 at epochs 10 and 20. The modality-specific loss weight λ and distillation weight β are set to 0.3 and 0.08, respectively, based on the validation set. For fair comparison, we fix the replay buffer size to 320 for all replay-based methods. All experiments are implemented in PyTorch, conducted on a single NVIDIA RTX 3090 GPU, and follow the continual learning protocol of PyCIL [38]. For evaluation, MoAS is applied only to novelty detection, whereas known-class classification is performed using the main logits.

4.2. Comparison Results

Novel Activity Detection Results. We compare MAND against all combinations of CL methods and novelty scoring methods across all three sequence-length settings. Table 1 reports the novelty detection performance of each CL-scoring pair. MAND achieves the best results in all three settings, outperforming even the strongest baseline pairs, such as MaxLogit or Energy combined with ER or iCaRL. Compared with the best baseline combination, MAND improves AUC by 9.6% and reduces FPR95 by 33.9% on average across the three settings. We further present the task-wise performance trends of the best-performing baseline pairs in Fig. 3. As shown in Figure 3, the performance gains of MAND are maintained throughout most of the task stream. We attribute these gains to more reliable modality-aware novelty scoring enabled by stabilizing modality-specific representations over continual updates.

Known-Class Classification Results. Table 2 and Figure 4 compare known-class classification performance across the

Table 1. Novel activity detection results on UESTC-MMEA-CL across all combinations of CL methods and novelty scoring functions under three class-incremental settings. Higher is better for AUC_T (\uparrow), and lower is better for $FPR95_T$ (\downarrow). Results are reported as mean \pm std over 5 runs. $\blacktriangledown/\blacktriangle$ indicates statistically worse/better performance than the proposed method according to a Wilcoxon signed-rank test ($p < 0.05$).

Method		Short Seq. (Inc: 8)		Mid Seq. (Inc: 4)		Long Seq. (Inc: 2)	
		AUC_T (\uparrow)	$FPR95_T$ (\downarrow)	AUC_T (\uparrow)	$FPR95_T$ (\downarrow)	AUC_T (\uparrow)	$FPR95_T$ (\downarrow)
iCaRL [32]	MSP [16]	85.92 \pm 0.84 \blacktriangledown	57.86 \pm 2.15 \blacktriangledown	84.51 \pm 0.68 \blacktriangledown	63.83 \pm 1.68 \blacktriangledown	81.33 \pm 0.86 \blacktriangledown	66.60 \pm 2.39 \blacktriangledown
	MaxLogit [17]	84.80 \pm 0.95 \blacktriangledown	59.65 \pm 4.85 \blacktriangledown	84.66 \pm 1.03 \blacktriangledown	64.60 \pm 1.24 \blacktriangledown	82.18 \pm 1.03 \blacktriangledown	64.22 \pm 2.89 \blacktriangledown
	Entropy [3]	85.69 \pm 0.85 \blacktriangledown	55.35 \pm 1.68 \blacktriangledown	85.02 \pm 0.64 \blacktriangledown	60.43 \pm 1.36 \blacktriangledown	81.75 \pm 0.67 \blacktriangledown	63.94 \pm 2.36 \blacktriangledown
	Energy [27]	84.62 \pm 0.97 \blacktriangledown	61.56 \pm 5.28 \blacktriangledown	84.49 \pm 1.05 \blacktriangledown	65.54 \pm 1.54 \blacktriangledown	82.06 \pm 1.05 \blacktriangledown	65.67 \pm 2.68 \blacktriangledown
ER [4]	MSP [16]	84.04 \pm 0.36 \blacktriangledown	59.63 \pm 2.06 \blacktriangledown	82.61 \pm 1.08 \blacktriangledown	66.13 \pm 2.26 \blacktriangledown	80.02 \pm 0.67 \blacktriangledown	69.35 \pm 0.74 \blacktriangledown
	MaxLogit [17]	86.37 \pm 0.79 \blacktriangledown	57.55 \pm 5.18 \blacktriangledown	85.06 \pm 0.90 \blacktriangledown	62.51 \pm 3.03 \blacktriangledown	82.02 \pm 1.01 \blacktriangledown	67.02 \pm 1.32 \blacktriangledown
	Entropy [3]	84.38 \pm 0.30 \blacktriangledown	58.12 \pm 2.28 \blacktriangledown	82.94 \pm 1.09 \blacktriangledown	64.21 \pm 1.68 \blacktriangledown	80.41 \pm 0.65 \blacktriangledown	67.63 \pm 0.84 \blacktriangledown
	Energy [27]	86.22 \pm 0.79 \blacktriangledown	58.87 \pm 5.15 \blacktriangledown	84.90 \pm 0.88 \blacktriangledown	63.73 \pm 2.85 \blacktriangledown	81.79 \pm 1.01 \blacktriangledown	67.90 \pm 1.19 \blacktriangledown
DER++ [2]	MSP [16]	82.05 \pm 0.97 \blacktriangledown	64.80 \pm 1.53 \blacktriangledown	81.68 \pm 1.03 \blacktriangledown	70.24 \pm 2.21 \blacktriangledown	78.43 \pm 0.68 \blacktriangledown	73.33 \pm 0.82 \blacktriangledown
	MaxLogit [17]	81.79 \pm 1.00 \blacktriangledown	66.65 \pm 4.02 \blacktriangledown	81.92 \pm 1.48 \blacktriangledown	69.79 \pm 2.08 \blacktriangledown	74.11 \pm 1.31 \blacktriangledown	82.81 \pm 1.73 \blacktriangledown
	Entropy [3]	82.67 \pm 1.01 \blacktriangledown	60.36 \pm 2.52 \blacktriangledown	82.33 \pm 1.09 \blacktriangledown	67.02 \pm 2.53 \blacktriangledown	78.99 \pm 0.71 \blacktriangledown	71.03 \pm 1.00 \blacktriangledown
	Energy [27]	81.48 \pm 1.03 \blacktriangledown	68.07 \pm 4.17 \blacktriangledown	81.65 \pm 1.49 \blacktriangledown	71.45 \pm 2.42 \blacktriangledown	73.56 \pm 1.33 \blacktriangledown	84.63 \pm 1.77 \blacktriangledown
Foster [33]	MSP [16]	83.81 \pm 0.82 \blacktriangledown	60.41 \pm 1.21 \blacktriangledown	80.85 \pm 0.49 \blacktriangledown	68.26 \pm 1.07 \blacktriangledown	76.57 \pm 0.46 \blacktriangledown	72.20 \pm 2.17 \blacktriangledown
	MaxLogit [17]	83.76 \pm 1.02 \blacktriangledown	60.95 \pm 2.50 \blacktriangledown	81.65 \pm 0.40 \blacktriangledown	71.97 \pm 0.70 \blacktriangledown	76.90 \pm 0.42 \blacktriangledown	77.84 \pm 2.01 \blacktriangledown
	Entropy [3]	84.14 \pm 0.76 \blacktriangledown	58.67 \pm 0.52 \blacktriangledown	81.39 \pm 0.49 \blacktriangledown	66.78 \pm 1.03 \blacktriangledown	77.21 \pm 0.45 \blacktriangledown	71.55 \pm 1.41 \blacktriangledown
	Energy [27]	83.61 \pm 1.06 \blacktriangledown	62.70 \pm 2.77 \blacktriangledown	81.44 \pm 0.37 \blacktriangledown	73.26 \pm 0.74 \blacktriangledown	76.34 \pm 0.41 \blacktriangledown	79.78 \pm 1.87 \blacktriangledown
CMR-MFN [34]	MSP [16]	70.86 \pm 0.60 \blacktriangledown	79.23 \pm 1.22 \blacktriangledown	67.58 \pm 0.78 \blacktriangledown	85.69 \pm 1.18 \blacktriangledown	58.70 \pm 0.82 \blacktriangledown	89.08 \pm 0.87 \blacktriangledown
	MaxLogit [17]	79.40 \pm 0.33 \blacktriangledown	70.60 \pm 1.39 \blacktriangledown	73.29 \pm 0.63 \blacktriangledown	81.25 \pm 1.77 \blacktriangledown	63.34 \pm 0.85 \blacktriangledown	84.59 \pm 1.40 \blacktriangledown
	Entropy [3]	78.38 \pm 0.35 \blacktriangledown	70.74 \pm 0.75 \blacktriangledown	71.38 \pm 0.58 \blacktriangledown	79.80 \pm 1.35 \blacktriangledown	59.67 \pm 1.09 \blacktriangledown	86.79 \pm 1.92 \blacktriangledown
	Energy [27]	79.43 \pm 0.37 \blacktriangledown	70.94 \pm 1.68 \blacktriangledown	73.20 \pm 0.71 \blacktriangledown	81.44 \pm 2.06 \blacktriangledown	63.60 \pm 0.81 \blacktriangledown	83.75 \pm 1.01 \blacktriangledown
MONET [5]	MSP [16]	84.54 \pm 0.21 \blacktriangledown	59.40 \pm 1.92 \blacktriangledown	83.39 \pm 0.56 \blacktriangledown	66.72 \pm 0.52 \blacktriangledown	80.07 \pm 0.55 \blacktriangledown	68.90 \pm 1.58 \blacktriangledown
	MaxLogit [17]	85.31 \pm 0.55 \blacktriangledown	62.35 \pm 3.93 \blacktriangledown	83.97 \pm 0.75 \blacktriangledown	65.18 \pm 1.64 \blacktriangledown	80.34 \pm 0.90 \blacktriangledown	68.12 \pm 2.44 \blacktriangledown
	Entropy [3]	84.81 \pm 0.26 \blacktriangledown	57.77 \pm 1.30 \blacktriangledown	83.73 \pm 0.61 \blacktriangledown	64.64 \pm 0.73 \blacktriangledown	80.43 \pm 0.57 \blacktriangledown	66.90 \pm 1.78 \blacktriangledown
	Energy [27]	85.06 \pm 0.61 \blacktriangledown	64.11 \pm 4.13 \blacktriangledown	83.81 \pm 0.75 \blacktriangledown	66.38 \pm 2.20 \blacktriangledown	80.17 \pm 0.92 \blacktriangledown	69.06 \pm 2.28 \blacktriangledown
MAND (Ours)	MAND (Ours)	95.20 \pm 0.24	23.02 \pm 1.97	94.79 \pm 0.52	25.75 \pm 2.46	92.32 \pm 1.51	36.48 \pm 7.04

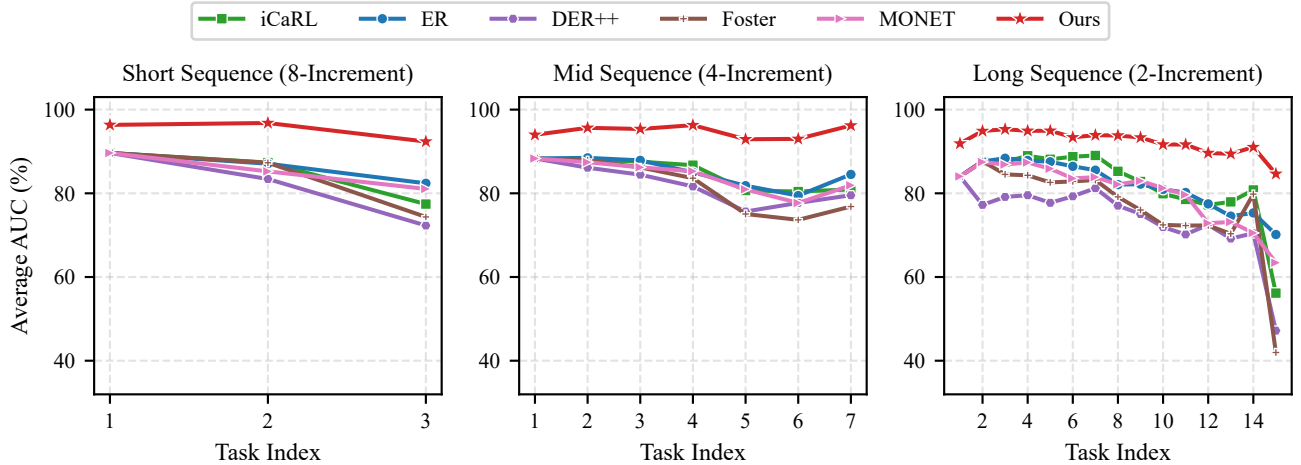


Figure 3. Task-wise novel activity detection performance. Average AUC over the task stream for the best-performing method pair in each class-incremental setting.

three class-incremental settings. MAND achieves the best average accuracy across all sequence lengths, outperforming strong replay-based baselines such as iCaRL and ER, with the performance margin becoming larger as more tasks accumulate. It also consistently reduces forgetting, achieving the

lowest forgetting in the long-sequence regime. This trend is consistent with Fig. 4, where MAND maintains higher accuracy throughout the task stream and degrades more slowly under the challenging 2-incremental setting. These results suggest that preserving modality-specific representations

Table 2. Known-class classification results on UESTC-MMEA-CL under three class-incremental settings. Higher is better for ACC_T (\uparrow), and lower is better for FGT_T (\downarrow). Results are reported as mean \pm std over 5 runs. $\blacktriangledown/\blacktriangle$ indicates statistically worse/better performance than the proposed method according to a Wilcoxon signed-rank test ($p < 0.05$).

Method	Short Seq. (Inc: 8)		Mid Seq. (Inc: 4)		Long Seq. (Inc: 2)	
	ACC_T (\uparrow)	FGT_T (\downarrow)	ACC_T (\uparrow)	FGT_T (\downarrow)	ACC_T (\uparrow)	FGT_T (\downarrow)
iCaRL [32]	85.96 ± 0.56	16.04 ± 0.93	$82.90 \pm 0.61\blacktriangledown$	$17.48 \pm 0.83\blacktriangledown$	$78.85 \pm 0.91\blacktriangledown$	20.71 ± 1.11
ER [4]	$84.76 \pm 1.29\blacktriangledown$	17.56 ± 1.49	$82.13 \pm 1.66\blacktriangledown$	$18.61 \pm 1.80\blacktriangledown$	$77.92 \pm 0.91\blacktriangledown$	$21.85 \pm 1.15\blacktriangledown$
DER++ [2]	$81.84 \pm 1.21\blacktriangledown$	15.00 ± 1.14	$79.16 \pm 1.02\blacktriangledown$	$18.31 \pm 1.27\blacktriangledown$	$75.15 \pm 1.59\blacktriangledown$	$23.05 \pm 1.49\blacktriangledown$
Foster [33]	$79.48 \pm 1.38\blacktriangledown$	$24.70 \pm 1.92\blacktriangledown$	$73.16 \pm 1.23\blacktriangledown$	$28.57 \pm 1.53\blacktriangledown$	$67.66 \pm 2.04\blacktriangledown$	$32.79 \pm 2.10\blacktriangledown$
CMR-MFN [34]	$75.25 \pm 1.40\blacktriangledown$	$13.16 \pm 1.31\blacktriangle$	$61.28 \pm 1.41\blacktriangledown$	14.10 ± 1.11	$26.40 \pm 2.07\blacktriangledown$	$22.25 \pm 1.91\blacktriangledown$
MONET [5]	$85.26 \pm 1.21\blacktriangledown$	17.03 ± 1.33	$82.29 \pm 1.04\blacktriangledown$	$18.42 \pm 1.18\blacktriangledown$	$78.83 \pm 1.01\blacktriangledown$	$21.01 \pm 1.02\blacktriangledown$
MAND (Ours)	86.66 ± 0.95	16.04 ± 1.58	85.67 ± 0.93	14.98 ± 1.09	81.56 ± 2.22	18.59 ± 2.08

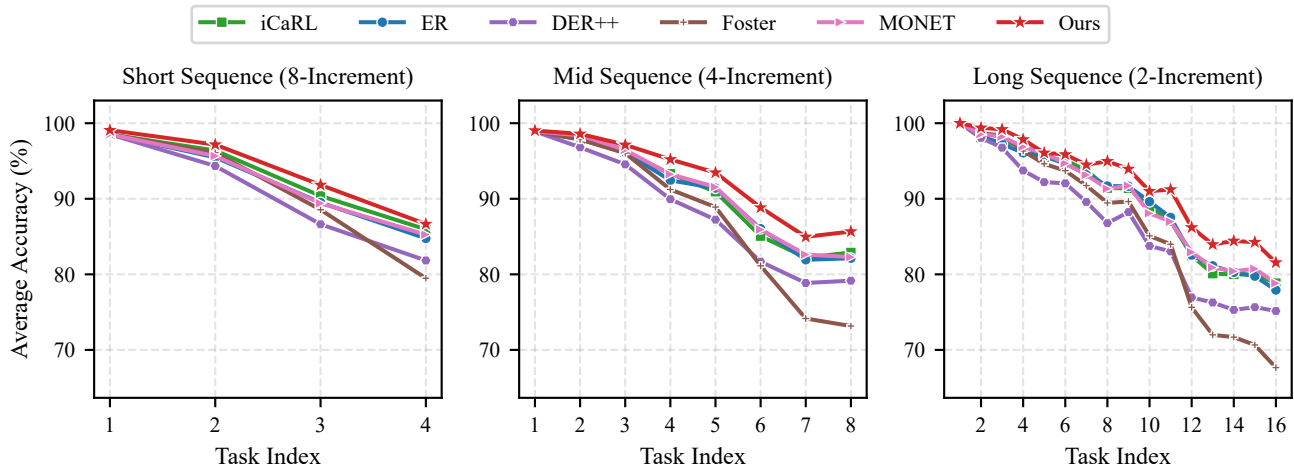


Figure 4. Task-wise known-class classification performance. Average accuracy over the task stream for continual learning methods under each class-incremental setting.

improves both knowledge retention and known-class classification in multimodal egocentric continual learning. Notably, the gains in known-class classification do not come at the expense of novelty detection, indicating that MAND improves stability and open-world adaptability simultaneously.

4.3. Ablation Study

Effect of the Proposed Modules. We conduct an ablation study to validate the contribution of each module in MAND. Table 3 reports both novel activity detection and known-class classification performance under three class-incremental settings. Removing MoAS leaves known-class classification nearly unchanged, which is consistent with its role as a novelty-scoring module, while consistently lowering AUC. In contrast, removing MoRST degrades both AUC and accuracy across all sequence lengths, with the largest accuracy drop in the mid-sequence setting. This highlights the importance of explicitly stabilizing modality-specific representations for both reliable novelty detection and ro-

bust known-class classification. Removing both MoAS and MoRST yields the lowest performance and reduces MAND to a level comparable to ER, confirming that the gains of MAND arise from the complementary roles of MoAS and MoRST.

Effect of the Scoring Strategy. To isolate the effect of adaptive reliability scoring, we compare MoAS against three fixed-weight baselines: Main Only, Uniform Sum, and Uniform Average, as defined in Tab. 4. The uniform strategies provide only marginal improvements over Main Only, indicating that naively aggregating modality logits is insufficient to exploit complementary modality cues effectively. In contrast, adaptive reliability achieves the best performance in all settings, improving AUC by more than 7% and reducing FPR95 by about 23% on average compared with the fixed-weight alternatives. This advantage is most pronounced in the long-sequence setting, where modality-specific forgetting across many incremental steps makes reliable modality-aware weighting increasingly important. Figure 5 visualizes

Table 3. Ablation results of the proposed modules for novel activity detection and known-class classification. Higher is better for AUC_T (\uparrow) and ACC_T (\uparrow).

Method	Short Seq. (Inc: 8)		Mid Seq. (Inc: 4)		Long Seq. (Inc: 2)	
	AUC_T (\uparrow)	ACC_T (\uparrow)	AUC_T (\uparrow)	ACC_T (\uparrow)	AUC_T (\uparrow)	ACC_T (\uparrow)
MAND	95.20 \pm 0.24	86.66 \pm 0.95	94.79 \pm 0.52	85.67 \pm 0.93	92.32 \pm 1.51	81.56 \pm 2.22
MAND w/o MoAS	87.50 \pm 0.61	86.66 \pm 0.95	87.33 \pm 0.81	85.67 \pm 0.93	84.04 \pm 0.72	81.56 \pm 2.22
MAND w/o MoRST	89.86 \pm 1.15	84.76 \pm 1.29	86.93 \pm 0.56	82.13 \pm 1.66	82.92 \pm 0.98	77.92 \pm 0.91
MAND w/o MoAS and MoRST	86.37 \pm 0.79	84.76 \pm 1.29	85.06 \pm 0.90	82.13 \pm 1.66	82.02 \pm 1.01	77.92 \pm 0.91

Table 4. Scoring strategy comparison for novel activity detection under three class-incremental settings. Higher is better for AUC_T (\uparrow), and lower is better for $FPR95_T$ (\downarrow).

Scoring Strategy	Short Seq. (Inc: 8)		Mid Seq. (Inc: 4)		Long Seq. (Inc: 2)	
	AUC_T (\uparrow)	$FPR95_T$ (\downarrow)	AUC_T (\uparrow)	$FPR95_T$ (\downarrow)	AUC_T (\uparrow)	$FPR95_T$ (\downarrow)
Main Only ($\alpha_m = 0$)	87.50 \pm 0.61	50.01 \pm 2.38	87.33 \pm 0.81	53.42 \pm 3.31	84.04 \pm 0.72	60.64 \pm 2.96
Uniform Sum ($\alpha_m = 1$)	87.85 \pm 0.68	46.50 \pm 2.46	88.17 \pm 0.41	51.57 \pm 2.46	84.46 \pm 1.36	58.78 \pm 4.33
Uniform Average ($\alpha_m = 1/\mathcal{M}$)	88.03 \pm 0.56	46.03 \pm 1.32	88.37 \pm 0.54	50.55 \pm 2.75	84.95 \pm 1.14	57.46 \pm 3.84
Adaptive Reliability (Ours)	95.20 \pm 0.24	23.02 \pm 1.97	94.79 \pm 0.52	25.75 \pm 2.46	92.32 \pm 1.51	36.48 \pm 7.04

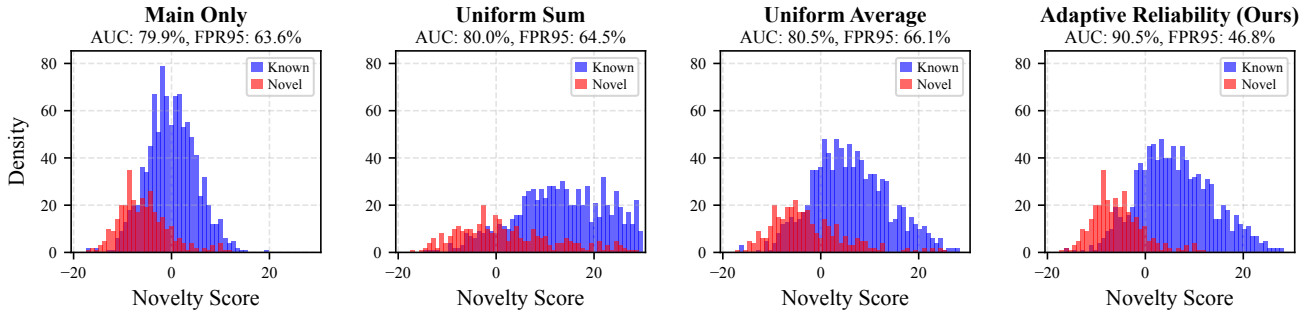


Figure 5. Effect of different scoring strategies on novelty score separability for Task 2 in the short-sequence (8-class incremental) setting.

the novelty score distributions under each strategy for Task 2 in the short sequence setting, which we use as a representative case where the overlap between Known and Novel samples is clearly visible. The uniform strategies broaden the score distributions relative to Main Only but do not meaningfully reduce the overlap between Known and Novel samples. In contrast, adaptive reliability scoring preserves the sharp peaks of both distributions while shifting them apart, resulting in a clear improvement in both AUC and FPR95.

5. Conclusion

In this study, we propose MAND, a modality-aware MMEA framework for OWCL, to address insufficient use of complementary modality evidence in novelty scoring and modality-wise instability under continual updates. MoAS improves separability between known and novel activities by adaptively weighting modality contributions at inference, while MoRST preserves per-modality discriminability through modality-specific supervision and replay-based logit distillation during training. Experiments show that MAND con-

sistently improves both novel activity detection and known-class classification, demonstrating the effectiveness of combining modality-aware scoring with modality-wise stabilization. A limitation of the current framework is the memory overhead introduced by stored modality logits and replay statistics, which may also be sensitive to buffer quality in long task streams. Future work will investigate more memory-efficient stabilization objectives and extend the framework to broader multimodal settings with varying sensor availability and stronger domain shifts.

References

- [1] Abhijit Bendale and Terrance Boult. Towards open world recognition. In *Proceedings of the IEEE Conference on Computer Vision and Pattern Recognition (CVPR)*, 2015. 2
- [2] Pietro Buzzega, Matteo Boschini, Angelo Porrello, Davide Abati, and SIMONE CALDERARA. Dark experience for general continual learning: a strong, simple baseline. In *Advances in Neural Information Processing Systems*, pages 15920–15930. Curran Associates, Inc., 2020. 5, 6, 7
- [3] Robin Chan, Matthias Rottmann, and Hanno Gottschalk.

- Entropy maximization and meta classification for out-of-distribution detection in semantic segmentation. In *Proceedings of the IEEE/CVF International Conference on Computer Vision (ICCV)*, pages 5128–5137, 2021. 5, 6
- [4] Arslan Chaudhry, Marcus Rohrbach, Mohamed Elhoseiny, Thalaiyasingam Ajanthan, Puneet K Dokania, Philip HS Torr, and Marc’Aurelio Ranzato. On tiny episodic memories in continual learning. *arXiv preprint arXiv:1902.10486*, 2019. 5, 6, 7
- [5] Evelyn Chee, Wynne Hsu, and Mong Li Lee. Monet: Multimodal online continual learning with novelty estimation. In *Proceedings of the IEEE/CVF International Conference on Computer Vision (ICCV) Workshops*, pages 5126–5135, 2025. 2, 3, 5, 6, 7
- [6] Chen Chen, Roozbeh Jafari, and Nasser Kehtarnavaz. Utdmhad: A multimodal dataset for human action recognition utilizing a depth camera and a wearable inertial sensor. In *2015 IEEE International Conference on Image Processing (ICIP)*, pages 168–172, 2015. 2
- [7] Shaoxu Cheng, Chiyuan He, Kailong Chen, Linfeng Xu, Hongliang Li, Fanman Meng, and Qingbo Wu. Vision-sensor attention based continual multimodal egocentric activity recognition. In *ICASSP 2024 - 2024 IEEE International Conference on Acoustics, Speech and Signal Processing (ICASSP)*, pages 6300–6304, 2024. 1, 2
- [8] Dima Damen, Hazel Doughty, et al. Rescaling egocentric vision: Collection, pipeline, and challenges for epic-kitchens-100. *International Journal of Computer Vision*, 130(1):33–55, 2022. 1, 2
- [9] Joseph DelPreto, Ching-Hsun Liu, et al. Actionsense: A multimodal dataset and recording framework for human activities using wearable sensors in a kitchen environment. In *Advances in Neural Information Processing Systems*, pages 13800–13813, 2022. 2
- [10] Jia Deng, Wei Dong, Richard Socher, Li-Jia Li, Kai Li, and Li Fei-Fei. Imagenet: A large-scale hierarchical image database. In *2009 IEEE Conference on Computer Vision and Pattern Recognition*, pages 248–255, 2009. 5
- [11] Jakob Engel, Kiran Somasundaram, Michael Goesele, Albert Sun, Alexander Gamino, Andrew Turner, Arjang Talattof, Arnie Yuan, Bilal Souti, Brighid Meredith, et al. Project aria: A new tool for egocentric multi-modal ai research. *arXiv preprint arXiv:2308.13561*, 2023. 1
- [12] Xinyu Gong, Sreyas Mohan, Naina Dhingra, Jean-Charles Bazin, Yilei Li, Zhangyang Wang, and Rakesh Ranjan. Mmg-ego4d: Multimodal generalization in egocentric action recognition. In *Proceedings of the IEEE/CVF Conference on Computer Vision and Pattern Recognition (CVPR)*, pages 6481–6491, 2023. 1
- [13] Kristen Grauman, Andrew Westbury, Eugene Byrne, et al. Ego4d: Around the world in 3,000 hours of egocentric video. In *Proceedings of the IEEE/CVF Conference on Computer Vision and Pattern Recognition (CVPR)*, pages 18995–19012, 2022. 1, 2
- [14] Meghna Gummadi, David Kent, Jorge A. Mendez, and Eric Eaton. Shels: Exclusive feature sets for novelty detection and continual learning without class boundaries. In *Proceedings of The 1st Conference on Lifelong Learning Agents*, pages 1065–1085. PMLR, 2022. 2
- [15] Chiyuan He, Shaoxu Cheng, Zihuan Qiu, Linfeng Xu, Fanman Meng, Qingbo Wu, and Hongliang Li. Continual egocentric activity recognition with foreseeable-generalized visual–imu representations. *IEEE Sensors Journal*, 24(8):12934–12945, 2024. 1, 2
- [16] Dan Hendrycks and Kevin Gimpel. A baseline for detecting misclassified and out-of-distribution examples in neural networks. *arXiv preprint arXiv:1610.02136*, 2016. 5, 6
- [17] Dan Hendrycks, Steven Basart, Mantas Mazeika, Andy Zou, Joseph Kwon, Mohammadreza Mostajabi, Jacob Steinhardt, and Dawn Song. Scaling out-of-distribution detection for real-world settings. In *Proceedings of the 39th International Conference on Machine Learning*, pages 8759–8773. PMLR, 2022. 5, 6
- [18] Sergey Ioffe and Christian Szegedy. Batch normalization: Accelerating deep network training by reducing internal covariate shift. In *Proceedings of the 32nd International Conference on Machine Learning*, pages 448–456, Lille, France, 2015. PMLR. 5
- [19] K. J. Joseph et al. Towards open world object detection. In *Proceedings of the IEEE/CVF Conference on Computer Vision and Pattern Recognition (CVPR)*, pages 5830–5840, 2021. 2
- [20] Evangelos Kazakos, Arsha Nagrani, Andrew Zisserman, and Dima Damen. Epic-fusion: Audio-visual temporal binding for egocentric action recognition. In *Proceedings of the IEEE/CVF International Conference on Computer Vision (ICCV)*, 2019. 3, 5
- [21] Gyuhak Kim, Changnan Xiao, Tatsuya Konishi, Zixuan Ke, and Bing Liu. A theoretical study on solving continual learning. In *Advances in Neural Information Processing Systems*, 2022. 2
- [22] Gyuhak Kim, Changnan Xiao, Tatsuya Konishi, Zixuan Ke, and Bing Liu. Open-world continual learning: Unifying novelty detection and continual learning. *Artificial Intelligence*, 338:104237, 2025. 1, 2, 3, 5
- [23] James Kirkpatrick, Razvan Pascanu, Neil Rabinowitz, Joel Veness, Guillaume Desjardins, Andrei A. Rusu, Kieran Milan, John Quan, Tiago Ramalho, Agnieszka Grabska-Barwinska, Demis Hassabis, Claudia Clopath, Dharshan Kumaran, and Raia Hadsell. Overcoming catastrophic forgetting in neural networks. *Proceedings of the National Academy of Sciences*, 114(13):3521–3526, 2017. 2
- [24] Yujie Li, Xin Yang, Hao Wang, Xiangkun Wang, and Tianrui Li. Learning to prompt knowledge transfer for open-world continual learning. *Proceedings of the AAAI Conference on Artificial Intelligence*, 38(12):13700–13708, 2024. 1, 2, 3, 5
- [25] Zhizhong Li and Derek Hoiem. Learning without forgetting. *IEEE Transactions on Pattern Analysis and Machine Intelligence*, 40(12):2935–2947, 2018. 2
- [26] Bing Liu, Sahisnu Mazumder, Eric Robertson, and Scott Grigsby. Ai autonomy: Self-initiated open-world continual learning and adaptation. *arXiv preprint arXiv:2203.08994*, 2022. 2
- [27] Weitang Liu, Xiaoyun Wang, John D. Owens, and Yixuan Li. Energy-based out-of-distribution detection. In *Proceedings*

of the 34th International Conference on Neural Information Processing Systems, Red Hook, NY, USA, 2020. Curran Associates Inc. 5, 6

- [28] Michael McCloskey and Neal J Cohen. Catastrophic interference in connectionist networks: The sequential learning problem. In *Psychology of learning and motivation*, pages 109–165. Elsevier, 1989. 2
- [29] Adrián Núñez-Marcos, Gorka Azkune, and Ignacio Arganda-Carreras. Egocentric vision-based action recognition: A survey. *Neurocomputing*, 472:175–197, 2022. 1
- [30] Ferda Ofli, Rizwan Chaudhry, Gregorij Kurillo, René Vidal, and Ruzena Bajcsy. Berkeley mhad: A comprehensive multimodal human action database. In *2013 IEEE Workshop on Applications of Computer Vision (WACV)*, pages 53–60, 2013. 2
- [31] Francisco Javier Ordóñez and Daniel Roggen. Deep convolutional and lstm recurrent neural networks for multimodal wearable activity recognition. *Sensors*, 16(1), 2016. 5
- [32] Sylvestre-Alvise Rebuffi, Alexander Kolesnikov, Georg Sperl, and Christoph H Lampert. icarl: Incremental classifier and representation learning. In *Proceedings of the IEEE conference on Computer Vision and Pattern Recognition*, pages 2001–2010, 2017. 2, 5, 6, 7
- [33] Fu-Yun Wang, Da-Wei Zhou, Han-Jia Ye, and De-Chuan Zhan. Foster: Feature boosting and compression for class-incremental learning. In *Computer Vision – ECCV 2022*, pages 398–414, Cham, 2022. Springer Nature Switzerland. 5, 6, 7
- [34] Hanxin Wang, Shuchang Zhou, Qingbo Wu, Hongliang Li, Fanman Meng, Linfeng Xu, and Heqian Qiu. Confusion mixup regularized multimodal fusion network for continual egocentric activity recognition. In *2023 IEEE/CVF International Conference on Computer Vision Workshops (ICCVW)*, pages 3552–3561, 2023. 2, 5, 6, 7
- [35] Yi Wang, Yi Ding, Xiangjian He, Xin Fan, Chi Lin, Fengqi Li, Tianzhu Wang, Zhongxuan Luo, and Jiebo Luo. Novelty detection and online learning for chunk data streams. *IEEE Transactions on Pattern Analysis and Machine Intelligence*, 43(7):2400–2412, 2021. 2
- [36] Linfeng Xu, Qingbo Wu, Lili Pan, Fanman Meng, Hongliang Li, Chiyuan He, Hanxin Wang, Shaoxu Cheng, and Yu Dai. Towards continual egocentric activity recognition: A multimodal egocentric activity dataset for continual learning. *IEEE Transactions on Multimedia*, 26:2430–2443, 2024. 1, 2, 3, 5
- [37] Friedemann Zenke, Ben Poole, and Surya Ganguli. Continual learning through synaptic intelligence. In *Proceedings of the 34th International Conference on Machine Learning*, pages 3987–3995. PMLR, 2017. 2
- [38] Da-Wei Zhou, Fu-Yun Wang, Han-Jia Ye, and De-Chuan Zhan. Pycil: a python toolbox for class-incremental learning. *SCIENCE CHINA Information Sciences*, 66(9):197101, 2023. 5